



A spectrally integrated temporal albedo model for thin composite layers of snow and ice on roads
by Andrew Gregory Beddoe

A thesis submitted in partial fulfillment of the requirements for the degree of Master of Science in
Mechanical Engineering
Montana State University
© Copyright by Andrew Gregory Beddoe (2001)

Abstract:

This study presents a spectrally integrated solar albedo model for thin composite layers of snow, ice and water on roads. The model is intended to support micro-scale thermal mapping models for forecasting highway pavement temperatures and surface conditions.

The snow-on-slab albedo (SOSA) model estimates the temporal road albedo by modeling surface conditions on highways that strongly affect solar albedo. Snow grain size, impurity concentration and optical mass were found to be important factors. These three factors were highly influenced by traffic and winter maintenance operations.

SOSA is composed of two components (1) a computation albedo routine CAR and (2) a pavement snow conditions routine SCR. CAR calculates visible, near infrared and solar albedos (0.3 - 5 μm) from 7 physically based parameters: snow grain radius (μm), carbon soot concentration (mass fraction), mass cross-section (g/cm^2), zenith cosine, atmospheric pressure (millibar), underlying surface albedo, diffuse fraction, surface downflux and atmospheric transmittance. SCR models the optical mass of water, ice, snow and sand, light absorbing impurities and the optical grain size. Inputs to SCR are meteorological parameters, surface energy fluxes and traffic parameters.

The optically equivalent grain size required in the model was 1/10th the observed grain size, partially due to the measurement protocol, which classified particle size by the longest dimension. Optical radii ranged from 50- 150 μm . The sanding materials were the principle light absorbing impurity. Carbon residue from vehicle exhaust and tire residue was insignificant. The sanding material was composed primarily of basalt and granite and had $\sim 0.07\%$ the optical influence of carbon soot in the model. The 0.07% normalization factor is related to the ratio of the imaginary indices of refraction between carbon soot and the bulk sanding material.

Despite erratic and quickly changing surface conditions, SOSA proved effective in calculating albedo. SOSA had an overall standard deviation of 0.15 from observed albedos for the entire road and shoulder. The accuracy of the model improved when it was restricted to calculate albedos inside the lanes only. The standard deviation decreased to 0.11. As a result SOSA estimated surface temperatures accurately over a 24hr period. Surface temperature standard deviations were less than 1.7°C from measured values.

A SPECTRALLY INTEGRATED TEMPORAL ALBEDO MODEL
FOR THIN COMPOSITE LAYERS OF
SNOW AND ICE ON ROADS

by

Andrew Gregory Beddoe

A thesis submitted in partial fulfillment
of the requirements for the degree

of

Master of Science

in

Mechanical Engineering

MONTANA STATE UNIVERSITY – BOZEMAN
Bozeman, Montana

November 29, 2001

© COPYRIGHT

by

Andrew Gregory Beddoe

2001

All Rights Reserved

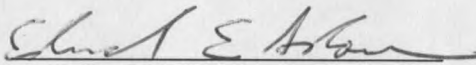
N378
B3899

APPROVAL

Of a thesis submitted by
Andrew Gregory Beddoe

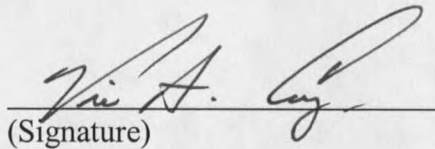
This thesis has been read by each member of the thesis committee and has been found to be satisfactory regarding content, English usage, format, citations, bibliographic style, and consistency, and is ready for submission to the College of Graduate Studies.

Dr. Edward E. Adams

 29-NOV-2001
(Signature) Date

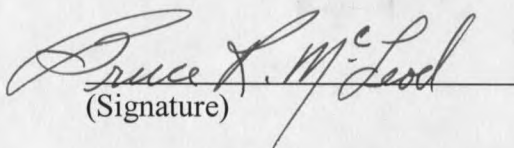
Approved for the Department of Mechanical Engineering

Dr. Vic A. Cundy

 11/29/01
(Signature) Date

Approved for the College of Graduate Studies

Dr. Bruce McLeod

 12-3-01
(Signature) Date

STATEMENT OF PERMISSION TO USE

In presenting this thesis in partial fulfillment of the requirements for a master's degree at Montana State University – Bozeman, I agree that the library shall make it available to borrowers under rules of the Library.

If I have indicated my intention to copyright this thesis by including a copyright notice page, copying is allowable only for scholarly purposes, consistent with "fair use" as prescribed in the U.S. Copyright Law. Requests for permission for extended quotation from or reproduction of this thesis (paper) in whole or in parts may be granted only by the copyright holder.

Signature Andrew Bedore

Date 11/30/2001

ACKNOWLEDGEMENTS

I would like to thank the Western Transportation Institute for providing the opportunity to conduct the research through their generous financial support via the Safe Passage project, as well as for scholastic assistance provided through the transportation graduate fellowship and graduate research assistantship. Special thanks to Dr. Edward Adams for his leadership, guidance and mentorship. Also, thanks to all others who provided their personal insight and recommendations, Dr. John Mounce, Dr. Douglas Cairns, Dr. Robert Brown, Dr. Jay Conant and Dr. Vic Cundy. Finally, a special thanks to my wife Mary Beddoe and other family members for their enduring support and love.

TABLE OF CONTENTS

1. INTRODUCTION	1
2. BACKGROUND	7
RADIATION	9
Shortwave Radiation.....	9
Absorption and Scattering by Particles.....	14
ALBEDO	21
Pavement.....	23
Snow	23
Spectral Albedo.....	24
Cloud Cover.....	25
Grain Size.....	27
Liquid Water.....	27
Light Absorbing Impurities.....	28
Snow Depth.....	31
THEORETICAL MODEL OF SNOW ALBEDO.....	33
PARAMETERIZATION OF SNOW ALBEDO	37
Parameters.....	39
Effective Grain Size Parameter.....	39
Effective Soot Parameter	41
Atmospheric Transmittance	42
Diffuse Fraction Parameter	43
Snow Albedo Parameterization.....	45
Clear Sky Albedo.....	45
Near-Infrared Albedo Under Cloudy Skies	47
Extension of Near-Infrared to 5 μm	47
SNOW ON ROADS	48
Winter Maintenance Practices	48
Vehicle Influences	52
Characteristics of Snow on Roads	53
3. METHODOLOGY	57
INSTRUMENTS AND OBSERVATIONS.....	57
Radiation Instrumentation.....	63
Pyranometers.....	63
Pyradiometer.....	66

Observations	67
Snow Grain Size	67
Snow Depth.....	68
SNOW-ON-SLAB ALBEDO MODEL	69
Computational Albedo Routine.	70
Pavement Snow Conditions Routine.	76
Effective Grain Size.....	76
The Optical Mass Cross-Section.....	77
Test-Platform	82
Longwave Radiation Flux.....	84
Shortwave Radiation Flux.....	85
Turbulent Fluxes	85
Ground Heat Flux	90
Precipitation Heat Flux	93
Vehicle Heat Flux	93
4. RESULTS AND FINDINGS.....	94
RESULTS	94
Albedo.....	94
Snowcover Properties	98
Traffic and Winter Operations.....	102
FINDINGS	108
Validation of the Computational Albedo Routine (CAR)	108
Determining the Optical Grain Size in the Model	110
Determining the Effective Soot Content in the Model	114
Validation of the Test-Platform	124
Temporal Snow-on-Slab Albedo Model.....	131
5. CONCLUSIONS AND RECOMMENDATIONS	144
REFERENCES	148
APPENDIX A: SNOW-ON-SLAB ALBEDO MODEL SOURCE CODE	156

LIST OF TABLES

Table	Page
1. Solar radiation wavelength regions and respective mean radiation energy. The wavelength separation between VIS and NIR for radiative transfer models is generally divided at 0.7 or 0.9 μm . ARPS makes the separation at 0.7 μm . Reproduced from Pluss [1997].	13
2. VIS wavelength regions and the corresponding colors. Reproduced from Table 1.4, Kondratyev [1969].	13
3. Parameters affecting albedo and emissivity of snow. Reproduced from Table 2, Warren [1982].	24
4. Geometrical depth of snow on a surface for various densities of snow vs. arbitrary critical depths. The geometrical depth d_s is estimated from $d_s = C_d/\rho$ where C_d is the critical depth and ρ is the median density of the snow. LED refers to the liquid equivalent depth. The median density for each snow classification is estimated from Table 1, Maeno et al. [1988].	32
5. Values of slope used to estimate an effective grain radius in equation (18). Reproduced from Table 2.2, Marshall [1989].	41
6. Values of coefficients from equation (19) and (20) for VIS and NIR spectral regions. Reproduced from Table 2.3, Marshall [1989].	42
7. Values of the coefficients a and b in equation (24) f' and g' in (26) and c and k in (28) for VIS and NIR spectral regions. Reproduced from Table 2.4, Marshall [1989].	44
8. Values for the coefficients a, b, c and d in equation (29) and (30) for spectral regions VIS and NIR. Reproduced from Table 2.5, Marshall [1989].	45
9. Values for the slopes k_{h1} , k_{h2} and k_l in equations (32), (33) and (38), coefficients a, b, c and d from (36) and (37), and coefficients e and f from (35). Reproduced from Table 2.6 and 2.7, Marshall [1989].	46
10. Values of the coefficients a', b' and c' in equation (39), and a, b and c in equation (41). Reproduced from Table 2.8, Marshall [1989].	47

11. Gradation of sanding aggregate. Montana test method MT-202.	51
12. Classification of snow and ice on roads. Reproduced from Table 1, Maeno et al. [1988].	55
13. Instruments on the RWIS used for this study.	59
14. Three divisions noted on road.	60
15. Snow Classification and median densities.	61
16. Estimating median depth of water on road.	68
17. Effective snow grain radius with respect to FWC. The effective radius is adopted from radii used by WWI and WWII to represent new, aged and melting snow.	76
18. General classification of precipitation rates based on intensity classifications by the NWS.	80
19. Traffic erosion rates verses FWC of snow. The ρ_s was taken near that of slush (900 kg/m^3) and AHT was taken as 50 veh/hr for $m_{xs} > 4.5 \text{ kg/m}^2$ and 100 veh/hr for $m_{xs} < 4.5 \text{ kg/m}^2$, where $m_{xs} = \rho_s \cdot d_s$. Δt was estimated from Figure 1, Schaerer [1970]. With $m_{xs} = 4.5$ and $\rho_s = 900 \text{ kg/m}^3$, d_s is $\sim 5 \text{ mm}$	81
20. Minimal mean wind speeds for turbulent conditions above the road surface. Characteristic lengths are taken as 10 m (represents wind perpendicular to 2 lane highway) and 40 m (wind parallel to highway). ν is for dry air, obtained from Appendix G, White [1991]. $Re_x =$ 500,000.	90
21. Winter operations frequency. %PlwFrqy refers to percent of passes in which plowing occurred. %SndFrqy refers to percent of passes in which sanding occurred.	103
22. Mean ADT for 1/23/01 to 4/25/01.	103
23. Comparison of weekend (wkend), weekday (wkday) and total week vehicle volumes. L1 and L2 refer to lane 1 and 2, respectively. CoVeh and PrVeh refer to commercial and private vehicle classification, respectively.	105
24. Average daily vehicles per hour. Average Vehicle per hour (Avg Hour), per period (Avg prd). The period is 15 minutes.	105

25. Coefficients a, b, c, d and e for equation (79).....	107
26. Snow grain radii obtained from snow pit work by Aoki et al. [2000]. r_1 is $\frac{1}{2}$ the longest length and r_2 is $\frac{1}{2}$ the shortest length the ice particle. Partially reproduced from Table 2, Aoki et al. [2000].....	112
27. STDs for Regions R1, R2, R3 with different normalization factors N_f	116
28. Spectral imaginary refractive index m_{im} ($\times 10^{-3}$) for basalt and granite. Granite is estimated from obsidian [Pollack et al. 1973].....	120
29. STDs for Regions R1, R2, R3 eliminating conditions with no snow.	122
30. Road conditions for February 5 th 2001. Measured data is from RWIS and predicted is from SOSA.	137
31. Road conditions for February 6 th 2001. Measured data is from RWIS and predicted is from SOSA.	142

LIST OF FIGURES

Figure	Page
1. SAFE-PASSAGE Corridor. BZH is located at mile marker 321.	10
2. Aerial photo of BZH	11
3. Angular distribution in Rayleigh and Mie scattering. Reproduced from Figure 3.3-6 Meyer-Arendt [1984].....	17
4. A plot of Rayleigh scattering intensity as a function of wavelength.	18
5. The influence of (a) grain radius, (b) zenith angle, (c) mass cross-section and (d) impurity concentration (soot) on the spectral albedo of snow. Reproduced from Figure 2.1, Marshall [1989].	26
6. The influence of (a) snow grain size, (b) solar zenith cosine, (c) snow mass cross-section and (d) impurity concentration of carbon soot on the spectrally integrated VIS (0.3 – 0.7 μm) and NIR (0.7-3 μm) snow albedo. The effective snow grain radius r is 1000 μm which represents old melting snow [Warren 1982]. Reproduced from Figure 2.2, Marshall [1989].....	40
7. RWIS at BZH.....	58
8. Hand held instrument and Li-Cor pyranometer sensor.....	62
9. Down facing pyranometer over I-90.....	63
10. LI-200SA spectra response curve. Reproduced from LI-COR radiation sensors instruction manual [1986].....	65
11. Spectral reflectivity of asphalt (bitumen) pavement. Partially duplicated from the Heat Island Group, http://EETD.LBL.gov/HeatIsland	65
12. The influence of snow grain size on albedo (a) for a $m_{xs} = 5 \text{ kg/m}^2$ and (b) for a $m_{xs} = 50 \text{ kg/m}^2$. Other data is $df = 0.5$, $patm = 750$ millibar, $\mu_o = 0.65$, $\alpha_g = 0.12$	71
13. Influence of the underlying surface on the albedo of thin snow over a range of grain sizes. Results for $m_{xs} = 0.5 \text{ kg/m}^2$, $df = 0.5$, $patm = 750$	

millibar, impurity concentration of 10 ppm and $\mu_0 = 0.65$. Pavement albedo varied from 1 to 0.	72
14. Influence of zenith cosine on snow albedo over a range of grain sizes. Results for $m_{xs} = 0.1 \text{ kg/m}^2$, $df = 0.5$, $p_{atm} = 750$ millibar impurity concentration of 10 ppm and 1000 ppm, $\alpha_g = 0.12$ and $\mu_0 = 0.65$	73
15. Influence of diffuse fraction on snow albedo over a range of grain sizes. Results for $m_{xs} = 0.1 \text{ kg/m}^2$, $df = 0.5$, $p_{atm} = 750$ millibar impurity concentration of 10 ppm and 1000 ppm, $\alpha_g = 0.12$ and $\mu_0 = 0.65$	74
16. Observed albedo on road for observation periods 2/5/01 through 3/30/01.	95
17. Measured albedo for different location on the road for observation periods 2/5/01 through 3/3/01.	96
18. Allwave albedo for (a) dry aged asphalt, (b) wet dry aged asphalt pavement, (c) dry sanding materials and (d) wet sanding materials.	97
19. Observed snow mass cross-section (g/cm^2) from 2/5/01 through 3/30/01.	99
20. Snow mass cross-section for different locations on road from 2/5/01 through 3/30/01.	99
21. Measured grain size for observation periods 2/5/01 through 3/30/01.	100
22. Observed impurity concentration (mass fraction) for observation periods 2/5/01 through 3/30/01.	101
23. Impurity concentration for R1, R2 and R3 for observation periods 2/5/01 through 3/30/01.	101
24. Average vehicles per hour by day of the week.	106
25. Average period traffic APT flow rates (vehicles per 15 minutes) for a typical (a) weekend and (b) weekday.	107
26. Measured vs. calculated albedo using CAR for wavelength separations between VIS and NIR (a) $0.9 \mu\text{m}$ and (b) $0.7 \mu\text{m}$. Data are for regions R1, R2, and R3.	109
27. Measured vs. calculated albedo, using CAR for different impurity fractions. Data are for WS 0.7 (a) 1% of measured grain size and (b) 10% of measured grain size. Regions R1, R2 and R3.	109

28. Measured vs. Calculated Albedo for VIS 0.7. Data represented is for (a) R1 (b) R2 and (c) R3. The normalization factor is taken as 1000, 1500 and 2000. (1) The influences of surrounding snow to raise the observed albedo above the calculated for bare asphalt. (2) The influence of surrounding bare pavement to lower the observed albedo below the calculated for snow.....117

29. Sanding materials compared to the respective color index.....119

30. Measured vs. Calculated Albedo for VIS 0.7 eliminating conditions with no snow. Data represented is for (a) overall road surface (b) R1 (c) R2 and (d) R3. The normalization factor Nf is taken as 1500.123

31. Measured vs. predicted surface temperatures for February 10, 2001.....126

32. Measured vs. predicted incoming IR radiation flux for February 10, 2001.126

33. Ground temperature at different depths. Data from 1/1/98 to 5/31/01.....127

34. Measured vs. predicted surface temperature for May 12, 2001.....128

35. Measured vs. predicted surface temperature for various n factors on May 12, 2001.....129

36. Measured vs. predicted surface temperature for an arbitrary n varied over the day, May 12, 2001.....129

37. Measured vs. predicted surface temperature for narps and nfit for February 10th, 2001.....130

38. SOSA results neglecting VEW for May 15th 2001. The plots are (a) surface temperature, (b) energy fluxes and (c) effective depth over the day.134

39. SOSA results including VEW for May 15th 2001. The plots are (a) surface temperature, (b) energy fluxes and (c) effective depth over the day.135

40. SOSA results including VEW for May 16th 2001. The plots are (a) surface temperature, (b) energy fluxes and (c) effective depth over the day.136

41. SOSA results including VEW for February 5th 2001. The plots are (a) surface temperature, (b) energy fluxes (c) effective depth and (d) albedo over the day.138

42. SOSA results including VEW for February 6th 2001. The plots are (a) surface temperature, (b) energy fluxes (c) effective depth and (d) albedo over the day.143

NOMENCLATURE

The following are the symbols used in the thesis

- A Cross-sectional control area (m^2).
- AHP Average hourly pass rate of winter maintenance vehicles.
- AHT Average vehicles per hour.
- APT Average vehicles per 15 minutes.
- B Thermal quality or fraction of ice in a unit mass of wet snow.
- C_p Specific heat (J/kg-K).
- d_f Diffuse fraction of solar downflux. Subscript c refers to clear sky diffuse fraction.
- d_s Geometrical snow depth (m).
- D_{oyr} Day of the year.
- E Amount of erosion. Subscripts v and m refer to vehicles and winter maintenance, respectively (kg/m^2).
- $e_{a,s}$ Water vapor pressure (kPa). Subscripts a and s refer to air and surface, respectively.
- f_{3-3} Fraction of near infrared flux from 3 to 5 μm .
- f_{basalt} Fraction of basalt in sanding materials.
- G Global irradiance (W/m^2). Sum of diffuse and direct solar radiation.
- g Gravitational acceleration (m/s^2).
- G_{xs} Geometrical cross-section (m^2).
- I Radiation flux (W/m^2). Subscript o stands for incident flux.
- k Boltzman molecular gas constant (J/molecule-K). Equation (42)
- k Thermal conductivity ($W/m-K$).

- k_e Extinction coefficient (m^{-1}). Subscripts a and s stand for absorption and scattering, respectively.
- $K_{h,e}$ Dimensionless turbulent heat transfer coefficient.
- L Latent heat of transformation (kJ/kg). Subscripts f, s and v refer to fusion, sublimation and vaporization, respectively.
- L Longwave radiation flux (W/m^2). Subscripts i and o refer to incident and emitted IR, respectively.
- M Amount of melting in snow layer (kg/m^2).
- m Mass (kg).
- m_{mol} Molar mass of air (kg/mol). Equation (42).
- $m_{re, im}$ Complex refractive index. Subscripts re and im stand for real and imaginary parts, respectively.
- m_{xs} Optical mass cross-section (kg/m^2).
- n Cloud cover fraction.
- N Number density (m^{-3}).
- n Number of particles. Equation (11).
- N_a Avogadro's number (molecules/kmol).
- N_f Normalization factor.
- P Amount of precipitation (kg/m^2).
- p Pressure (kPa or mmbar).
- P_i Precipitation intensity (m/s).
- Q Energy flux (W/m^2).
- R Gas constant (kJ/kg-K).
- r Particle radius (μm).
- R_{DAPT} Average diurnal vehicle flow rate (Vehicles / 15 minutes).

R_{ef}	Spectral reflectivity.
Re_x	Dimensionless Reynolds number.
S	Equivalent soot concentration of contaminate (mass-fraction).
t	Atmospheric transmittance.
Δt	time increment (seconds).
T	Temperature ($^{\circ}$ C).
U	Wind speed (m/s).
v	Velocity (m/s)
V	Volume (m^3).
WS	Wavelength separation between visible and near infrared regions (0.7 or 0.9 μm).
x	Optical path length or relative air mass (m).
x,y,z	Cartesian coordinates.
x_c	Characteristic length (m).
x_p	Characteristic size of scattering particle used in Mie Theory.
y	Elevation above reference pressure (m).
Z_e	Extinction efficiency. Subscripts a and s stand for absorption and scattering, respectively.
z_g	Nodal distance (m).
α	Albedo.
β	Attenuation coefficient (m^{-1})
ϵ	Surface emissivity.
ϵ	Internal energy per unit mass (J/kg). Equation (71).
θ	Zenith angle ($^{\circ}$).
Λ	Thermal diffusivity (m^2/s).

- λ Wavelength (m).
- μ_0 Cosine of the zenith angle.
- ν kinematic viscosity (m^2/s). Equation (68).
- ν Specific volume (m^3/kg). Equations (60) and (61).
- ρ Density (kg/m^3).
- σ Stefan-Boltzmann constant ($\text{W}/\text{m}^2\text{-K}^4$).
- σ_e Extinction cross-section (m^2). Subscripts a and s stand for absorption and scattering, respectively.
- τ_0 Optical snow depth.
- ϕ Relative humidity.

ABSTRACT

This study presents a spectrally integrated solar albedo model for thin composite layers of snow, ice and water on roads. The model is intended to support micro-scale thermal mapping models for forecasting highway pavement temperatures and surface conditions.

The snow-on-slab albedo (SOSA) model estimates the temporal road albedo by modeling surface conditions on highways that strongly affect solar albedo. Snow grain size, impurity concentration and optical mass were found to be important factors. These three factors were highly influenced by traffic and winter maintenance operations.

SOSA is composed of two components (1) a computation albedo routine CAR and (2) a pavement snow conditions routine SCR. CAR calculates visible, near infrared and solar albedos ($0.3 - 5 \mu\text{m}$) from 7 physically based parameters: snow grain radius (μm), carbon soot concentration (mass fraction), mass cross-section (g/cm^2), zenith cosine, atmospheric pressure (millibar), underlying surface albedo, diffuse fraction, surface downflux and atmospheric transmittance. SCR models the optical mass of water, ice, snow and sand, light absorbing impurities and the optical grain size. Inputs to SCR are meteorological parameters, surface energy fluxes and traffic parameters.

The optically equivalent grain size required in the model was $1/10^{\text{th}}$ the observed grain size, partially due to the measurement protocol, which classified particle size by the longest dimension. Optical radii ranged from $50 - 150 \mu\text{m}$. The sanding materials were the principle light absorbing impurity. Carbon residue from vehicle exhaust and tire residue was insignificant. The sanding material was composed primarily of basalt and granite and had $\sim 0.07\%$ the optical influence of carbon soot in the model. The 0.07% normalization factor is related to the ratio of the imaginary indices of refraction between carbon soot and the bulk sanding material.

Despite erratic and quickly changing surface conditions, SOSA proved effective in calculating albedo. SOSA had an overall standard deviation of 0.15 from observed albedos for the entire road and shoulder. The accuracy of the model improved when it was restricted to calculate albedos inside the lanes only. The standard deviation decreased to 0.11. As a result SOSA estimated surface temperatures accurately over a 24hr period. Surface temperature standard deviations were less than 1.7°C from measured values.

CHAPTER 1

INTRODUCTION

Winter driving conditions are hazardous and often confront motorists with extreme temporal and spatial variability because of local topography, traffic, maintenance practices and meteorological influences. Winter conditions also contribute a large economic burden in loss of property, time delays, and labor and material costs expended in winter maintenance operations [Hanbali 1992]. Many roads may see the highest injuries and fatalities during snowy and icy conditions in part due to the high variability of snow and ice on roads, which complicate anti-snow and ice measures [Naruse et al. 1987]. Knowing exactly when and where snow and/or ice will begin to melt or refreeze could improve planning, help cut costs of snow and ice control and reduce hazards for winter maintenance crews and road users. Because of this, motorists and traffic management personnel are in continual need of accurate real-time and forecasted road and weather conditions along rural roads and highways.

To assist in these efforts a more sophisticated snow albedo (reflectivity) model, controlled by the physical properties of snow, is needed for weather-related micro-forecast pavement temperature and condition models. A physically based albedo model will broaden the physical understanding and forecast accuracy of snow and ice formation and ablation on roads thus improving the effectiveness and deployment of anti-snow and ice measures. Albedo α plays a critical role in modeling efforts because it provides a quantitative measure of the fraction of incident solar radiation absorbed (e.g. fraction

absorbed = $1 - \alpha$) near the surface, and is the dominate energy available to cause increases in road surface temperatures and melt snow on roads during winter [Ishikawa et al. 1987, Naruse et al. 1988, Nakawa et al. 1992].

Albedo refers to the reflectivity of a surface (fraction of energy reflected) in the solar spectrum (generally between 0.2 to 5 μm). and is commonly parameterized as the spectrally-averaged (allwave) albedo. The word itself, albedo, in late latin means whiteness, from the latin albus (white).

Snow is an excellent reflector of shortwave (solar) radiation and emitter of longwave radiation. This means that snow usually lowers absorbed solar energy during the day while effectively emitting longwave radiation at night, creating a net radiation loss from a surface. These conditions commonly cause surface cooling which can lead to ice formation on the road surface.

The albedo of a snow covered road is the result of a composite structure of pavement, ice, anti-skid materials (sand aggregate) and snow acting in concert to absorb, scatter and reflect incident radiation. Of these, snow has the greatest influence on the observed albedo because of its high albedo (e.g. pure semi-infinite snow 0.7 to 0.85, [Marshall 1989]) as compared to dry asphalt (e.g. new asphalt has an albedo of 0.04 and aged asphalt ~5 to 10 years has a mean albedo of 0.12 ± 0.03 , [Pomerantz et al 1999]), water (e.g. an albedo of 0.06 for solar heights > 40 degrees, Fig 7.5, [Kondratyev 1969]) and common anti-skid abrasives (e.g. albedo of gray sand 0.18 to 0.23 , Table 7.3, [Kondratyev 1969]) used in winter maintenance.

It is apparent, then, that snow albedo has a enormous potential to change the amount of solar energy absorbed at the surface of the road. A change in snow albedo from 0.8 to 0.4 (e.g. from removal of snow by plowing or addition of light absorbing contaminants such as anti-skid materials) triples the amount of solar energy absorbed on the surface from 20% to 60% and may greatly accelerate melt [Naruse et al. 1988]. Even slight fluctuations in snow albedo may alter the onset of snowmelt or refreeze on the road, as indicated by Warren [1984] and Brown [1982] for undisturbed snow covers. Thus, an accurate knowledge of the surface albedo is required to precisely model when snowmelt and refreeze might occur.

Snow melting or aging generally has a positive feedback on the snow albedo. Albedo naturally decreases as snow ages because of snow grain growth and a decrease in snowcover thickness [Warren 1984]. As the albedo drops the snow cover is more efficient at absorbing solar energy which in turn increases ablation. This cycle is accelerated when traffic and winter maintenance are introduced and can rapidly change the snowcover conditions, which translates to a rapidly changing albedo [Ishikawa et al. 1987, Naruse et al. 1988]. Combined with dynamic solar effects from shadowing and thermal energy exchange between surfaces, particularly in mountainous regions, pavement temperatures and conditions during winter can fluctuate drastically along a road within a close distance.

Most snow albedo models to date have been developed for use in global climate modeling and were concerned only with natural snow covers experiencing seasonal metamorphism and ablation. The earliest albedo parameterizations treated albedo quite

crudely, generally prescribing snow albedo as a single value, or basing it on a distribution of the surface albedo [Marshall 1989]. Others have taken a simple parameterization of snow albedo, dependent on temperature, age of snow, zenith angle or latitude [Table 1.1, Marshall 1989]. However, many of the earlier parameterizations are derived from data at a single site and are not universal parameterizations, as published by Pluss [1997]. A more sophisticated approach was applied to model snow albedo by Marshall [1989], based on the sophisticated theoretical work of Wiscombe and Warren [1980a and 1980b, here after WWI and WWII]. Marshall [1989] developed simple functions, which accurately fit the spectrally integrated (allwave) results of the theoretical spectral albedo model. The model requires 7 realistic physically tuned inputs, which allows the parameterization to be transferable to other locations. However, the model is developed for use in atmospheric general circulation models (GCMs) and seasonal snowcovers and is not directly applicable to thin snow and ice covers on pavement where direct influences from anthropogenic sources must be considered.

Traffic and winter maintenance are factors that indirectly influence snow albedo on roads, but have not been considered at all in albedo models. Actions by vehicles and maintenance practices both alter the physical snow properties, thus snow albedo. Vehicles mechanically break snow crystals, compact snow, mix contaminants, move and erode snow on the road. Maintenance operations deposit large amounts of contaminants on the snow through application of abrasives and remove snow mass by plowing. In addition, differences in local traffic and anti-snow and ice operations contribute to the variable snow conditions along the road. The net result of these transportation influences

is to increase the inhomogeneity and to accelerate metamorphism and ablation of snow roads as compared to a seasonal snowpack, which complicates measuring and modeling efforts.

Within this thesis a allwave albedo model for thin composite layers of snow and ice on pavement (snow-on-slab) is presented. The albedo routine is adapted from a physically parameterized snow albedo model [Marshall 1989]. The snow-on-slab albedo (SOSA) model includes the effects from motor traffic and winter maintenance on the physical snow structure, contamination and ablation on pavement and is intended to support road surface temperature modeling efforts for snow and ice covered roads. The allwave albedo is calculated based on realistic physical conditions of the snowcover and the pavement.

This snow-on-slab albedo model is seen as necessary to improve the accuracy of pavement temperature forecasting. It provides the first ever (to the knowledge of the author) physically-based albedo model applied to snow and ice in a transportation setting. The model was developed to be incorporated into WinThermRT to improve albedo estimates to achieve more accurate forecast of surface temperatures (see Chapter 2). Improvements in surface temperature modeling will contribute to improved safety and efficiency on rural roads. Success of the thermal modeling will assist in increasing traveler safety through reduction in accidents, improve maintenance operations through effective and timely use of resources, and demonstrate the feasibility of ITS in rural applications.

The following summarize the rationale for the thesis:

1. The high variance of albedo of snow and ice on roads plays an important role in the surface energy budget.
2. Current classification of snow and ice on roads is lacking in a sophisticated approach in modeling albedo.
3. Future highway safety and efficiency will benefit from a physically – based albedo model tailored to road and highway snow.
4. Assist in development of intelligent transportation systems in rural settings.
5. Improve accuracy of strategic road weather and condition forecasting models.

CHAPTER 2

BACKGROUND

Support for this research was provided by the *Safe Passage* Project, a cooperative effort by the Western Transportation Institute (WTI), MSU-Bozeman and the Montana Department of Transportation (MDT). Funding was provided by the Research and Special Programs Administration of the U.S. Department of Transportation through WTI.

The *Safe Passage* Project is concerned with optimizing weather related operations, motorist safety and incident management along Interstate 90 (I-90), a major east-west corridor between Livingston and Bozeman (Figure 1). Severe weather conditions common in the northern rockies, that consistently plague the corridor during winter months, compel the project to focus on the issue of weather and weather-related pavement conditions, reported as contributing to up to 70% of the accidents between 1994-1999 [Accident statistics, MDT, Safety Management Section, 1998]. Intelligent Transportations Systems (ITS) technologies such as road and weather information systems (RWIS), employed in *Safe Passage*, provide site-specific meteorological and pavement temperature data, an important component to icing. However, it is economically impossible to line entire stretches of roads with sensors, thus requiring extrapolation between RWIS sites. This limits strictly using RWIS as decision support tools regarding appropriate action in snow and ice control efforts because of the limited accuracy of extrapolated pavement temperatures due to small amounts data between sites. As a result a micro-forecast pavement temperature model (WinThermRT) which utilizes

ITS technology in conjunction with National Weather Service (NWS) forecast data is in continuing development.

This thesis supports development of the computational thermal model (WinThermRT), an integral component of *Safe Passage*, which is intended to accurately micro-forecast pavement temperatures and roadway conditions. The thermal model (WinThermRT) is adapted from a computational model called PRISM (Physically Reasonable Infrared Signature Model) used by the U.S. Military to model surface temperatures of vehicles for use in infrared imagery [Adams and McDowell 1991]. PRISM uses a series of flat plates to represent the three-dimensional shape of a vehicle. Shadowing and surface to surface re-radiation are accounted for within the model. The concept was expanded to terrain and highways through employment of Geographic Information Systems (GIS) and Digital Elevation Maps (DEM) [Adams, WTI Report, Vol. 4 (1), March 2000].

Currently, WinThermRT micro-forecasts pavement temperatures to a 30 m resolution (Standard United States Geological Service (USGS) Dimensions) by extrapolating meteorological forecasted data (on a 40 km grid) obtained indirectly from the National Weather Service (NWS) and Eta program (a mesoscale meteorological model, for more detail contact the National Oceanic and Atmospheric Administration NOAA) via the Advanced Regional Prediction System [ARPS, Xue et al. 2000]. The albedo model was developed only as a point model within WinThermRT. The spatial extrapolation of albedo across the complex terrain grid is accomplished through WinThermRT's platform.

Therefore, the surface albedo at the grid point represents the averaged albedo for a 30 m square surface over the road.

Bozeman Hill (BZH) was chosen as the research site. It is located within the corridor at mile marker 321.1 (Figure 2). Only west bound lanes of I-90 were studied. Bozeman Hill was selected as the site because it provided the highest point along the highway within the corridor and is a good representative of the severe weather within the corridor or other mountain passes. Also, an existing MDT RWIS adjacent the highway helped reduce cost and construction time and provided an existing system into which additional radiation sensors could be integrated.

Radiation

Thermal models for pavement icing are primarily concerned with radiant energy exchange on a surface in the shortwave and longwave regions. Albedo is important in radiant energy exchange on surfaces because knowledge of albedo makes it possible to determine the amount of heat obtained from incoming shortwave (solar) radiation.

Shortwave Radiation

Radiation from the sun is the primary energy fueling atmospheric motions and different processes in the atmosphere, on the earth's surface and in the oceans [Kondratyev 1969, Pluss 1997]. Radiation emitted by the sun may be regarded as

